THE ASTROPHYSICAL JOURNAL, 215:781–787, 1977 August 1

THE CIRCUMSTELLAR ENVELOPE OF IRC +10216

JOHN KWAN AND F. HILL
State University of New York, Stony Brook
Received 1976 November 29

ABSTRACT

The circumstellar envelope of IRC +10216, a late-type carbon star, is modeled, and theoretical calculations of CO, ^{13}CO, HCN, and H^{13}CN emission are compared with observations. A steady mass loss from the star is assumed. The gas temperature in the flow is determined from considerations of the cooling due to free expansion and molecular emission, and the heating due to gas-dust collisions. The CO and ^{13}CO $J = 1 \rightarrow 0$ intensities are found to be insensitive to vibrational excitation by infrared photons. The HCN, H^{13}CN $J = 1 \rightarrow 0$ lines, on the other hand, depend primarily on vibrational excitation. The mass loss rate, deduced from the CO observations, is remarkably close to the limiting rate, for a flow driven by radiation pressure, of $\sim L/(cv_t)$, where L is the luminosity and v_t is the terminal velocity of the expanding gas. Assuming a distance of 200 pc to IRC +10216, the deduced mass loss rate is $2.10^{-5}\ M_\odot\ \mathrm{yr}^{-1}$ and the [CO]/[H_2] abundance ratio about $8 \cdot 10^{-4}$, both uncertain to a factor of 2. Comparing the CO with the ^{13}CO emission, a [CO]/[^{13}CO] isotope ratio of 35 ± 7 is obtained.

Subject headings: infrared: sources — stars: carbon — stars: circumstellar shells — stars: individual — stars: mass loss

I. INTRODUCTION

Millimeter wave molecular lines have been observed in emission toward many stars. The detected lines are usually masers of the OH, H_2O, or SiO molecule (cf. Snyder and Buhl 1975), except at IRC +10216, IRC +30219 (CIT-6), and IRC +40540 where thermal emission of CO has been observed (Wilson *et al.* 1971; Wilson, Schwartz, and Epstein 1973; Mufson and Liszt 1975; Frogel, Dickinson, and Hyland 1975). A common characteristic of all of these lines is the large velocity extent of the emission, which usually reaches 20 km s^{-1} or more. It is most simply interpreted as due to molecular emission in an expanding envelope. At IRC +10216, VY CMa, and NML Cyg, this interpretation is reinforced by the observation of CO vibration-rotational lines in absorption at a large negative velocity relative to the star (Geballe, Wollman, and Rank 1973). Several of the infrared absorption lines arise from high rotational levels of the ground vibrational state, and their observed intensities and velocities imply the presence, close to the star, of matter expanding at a high velocity. The detection of molecular emission from stars thus provides further evidence of mass loss from stars during their evolution.

Of the three stars where CO emission has been observed, IRC +10216 is the most thoroughly studied. This star has been identified as a late-type carbon star by Herbig and Zappala (1970). Infrared observations (Becklin *et al.* 1969; Toombs *et al.* 1972) show that the continuum radiation consists of two components: a 650 K blackbody of angular diameter 0".4, and an optically thin 2" shell at 350 K. Many molecular lines have been observed from this source. Ulich (1976) has mapped the extent of the CO emission and has measured its diameter at one-half peak intensity to be 140". Morris (1975), in analyzing the emission of SiS, SiO, CS, and HC_3N based on an expanding envelope model, concludes that excitation of these molecules by radiative absorption of the infrared continuum at vibration-rotational transitions is most important. Kuiper *et al.* (1976), from an empirical fit to their high-sensitivity CO and ^{13}CO line profiles, find that the observations are consistent with an expanding, partially resolved envelope, and optically thick CO emission and optically thin ^{13}CO emission.

In this paper we discuss a model for the circumstellar envelope of IRC +10216, assuming a steady mass loss from the star. The interpretation of the molecular emission as arising from an expanding spherical envelope leads to a simple procedure for analyzing the molecular observations. The velocity structure of the envelope is approximated well by a constant terminal velocity which can be estimated from the observed line width. The large expansion velocity gives rise to a large velocity gradient transverse to the radial direction, and enables a local solution of the molecular excitations, for which Sobolev's escape-probability formalism is especially suited. The density distribution with radius is known and scales with a single parameter, the mass loss rate. The temperature of the expanding gas can be determined, taking account of the cooling due to free expansion and molecular emission and the heating due to gas-dust collisions. Excitation of the molecular lines, as a result of both collisions and radiative absorption of infrared photons from the stellar continuum, can then be calculated and compared with observations, thereby obtaining information about the mass loss rate and the molecular abundances.

II. THE CIRCUMSTELLAR ENVELOPE

The circumstellar envelope is taken to extend from an inner radius of 2×10^{15} cm to beyond 5×10^{17} cm. The inner radius is specified mainly for computation purposes as a starting point for calculating the temperature distribution. Molecular emission from within 2×10^{15} cm contributes little to the observed intensities in the rotational lines of the ground vibrational state, except for instances of maser emission. The mass outflow is presumed to be due to radiation pressure on grains which form in the stellar atmosphere and which are momentum-coupled to the gas (Hoyle and Wickramasinghe 1962; Gilman 1969, 1972). The flow reaches the terminal velocity in essentially a few stellar radii. As far as calculating the density and temperature distributions and the escape probability for spontaneous emission is concerned, little error is committed in assuming the flow velocity to be constant beyond 2×10^{15} cm. However, in considering the absorption of infrared radiation at vibration-rotational frequencies, the radial velocity gradient, albeit small, can influence the number of photons absorbed when the line opacity to the continuum radiation becomes greater than unity. Because radiation pressure, gravity, and free expansion can all give rise to small accelerations of the flow, the velocity distribution beyond 2×10^{15} cm is largely a guess, and we shall assume $v(r) = v_t\,(1\text{–}4 \times 10^{14}\ \mathrm{cm}\ r^{-1})^{1/2}$. The effect of varying this distribution will be discussed along with the numerical calculations in the next section. The terminal velocity $v_t = 16.0\ \mathrm{km\ s^{-1}}$ is estimated from the observed CO emission (Kuiper *et al.* 1976) which extends over a velocity range of $32\ \mathrm{km\ s^{-1}}$.

The temperature of the gas as it expands depends on the cooling due to expansion, the cooling by molecular line emission, the heating from gas-dust collisions, and, to a much smaller extent, the heating due to radiative excitation to vibrational levels. The adiabatic index of the gas is taken to be 5/3. This is a good approximation, even for molecular hydrogen, at kinetic temperatures of less than 150 K. Molecular cooling is expected to be primarily due to CO line emission. Chemical equilibrium calculations by Dolan (1965) and Tsuji (1973) show that, next to H_2, CO is the most abundant molecule in the envelopes of carbon-rich giants or supergiants. We have verified that excitations of HCN, CS, and other observed molecules that are much less abundant than CO lead to negligible cooling. The effect of H_2 quadrupole emission is also calculated to be insignificant. Other molecules which might be abundant in the envelope but which have not been observed are CH and CH_2. Both are linear molecules (Herzberg 1966), and the simple structure of their rotational levels may not give rise to significant cooling, if the two molecules are less abundant than CO (Dolan 1965).

Collisions between hydrogen and dust grains provide an important source of heat for the gas in the expanding envelope (Goldreich and Scoville 1976). Because of radiation pressure on the grains, the latter maintain a drift velocity relative to the gas, such that momentum is effectively transferred from the grains to the gas (Gilman 1972). This drift velocity, v_d, is then approximately given by

$$\rho \sigma_d v_d^2 = \frac{L}{4\pi r^2 c}\,\sigma_d Q\,, \tag{1}$$

where ρ is the gas density, σ_d is the dust cross sectional area, L is the stellar luminosity, r is the distance from the star, and Q is the momentum transfer efficiency factor averaged over the spectral energy distribution of the continuum. Strictly, Q depends on r, since the dust grains constantly modify the emergent energy distribution. This spatial dependence is expected to be weak, and is not taken into account. The infrared continuum peaks at about 8 μm and Q determined at this wavelength would be roughly appropriate. However, this value is uncertain, and in the numerical calculations Q is regarded as a parameter which is varied. When writing equation (1), we assumed that, in determining the gas-dust collisional frequency, the drift velocity is greater than the gas thermal velocity. This approximation is good except close to the inner boundary. Rewriting equation (1),

$$v_d = \left(\frac{L v_t Q}{\dot{M} c}\right)^{1/2}, \tag{2}$$

where $\dot{M}$ denotes the mass loss rate. The integrated infrared flux observed from IRC +10216 is $1.7 \times 10^{-8}\ \mathrm{W\ m^{-2}}$ (Becklin *et al.* 1969) so that, at a distance d, the luminosity is $2.1 \times 10^4\ L_\odot\ (d/200\ \mathrm{pc})^2$.

As a result of the gas-dust drift, each time a particle collides with a dust grain it gains a kinetic energy of $\sim \frac{1}{2} m v_d^2$, so that the rate of heating per unit volume from this process is

$$\frac{dq}{dt}(\mathrm{dust}) = (n_{\mathrm{grain}} \sigma_d v_d)\tfrac{1}{2}\rho v_d^2\,. \tag{3}$$

The grains are assumed to constitute 1% by mass of the expanding matter, and have a radius of 0.1 μm and a density of $1\ \mathrm{g\ cm^{-3}}$. These values are estimates, but since they are always entered with Q, their uncertainties can also be entered into the uncertainty of Q. A check on the consistency of these parameters, however, can be made by calculating the dust optical depth and comparing it with that deduced from infrared observations.

Taking account of all the relevant cooling and heating processes, the rate of change of the gas temperature with radius can be written as:

$$\frac{dT}{dr} = -\frac{4T}{3r} - \frac{2}{3kv_t n}\frac{dq}{dt}(\mathrm{CO}) + \frac{2}{3kv_t n}\frac{dq}{dt}(\mathrm{dust})\,, \tag{4}$$

where n is the gas number density. In the second term on the right-hand side of equation (4), $dq(\mathrm{CO})/dt$ represents the time rate of energy loss per unit volume due to CO line emission. The effect of vibrational excitation is included in this term. In the numerical calculations, an initial gas temperature of 350 K is assumed at 2×10^{15} cm. In the inner parts of the

envelope cooling due to expansion and CO emission quickly lowers the temperature of the gas as it expands. Over the outer parts of the envelope where most of the molecular emission occurs, the gas temperature is insensitive to the initial temperature assumed at 2×10^{15} cm.

In calculating the molecular emission, we shall be concerned only with the molecules CO, ^{13}CO, HCN, and H^{13}CN. Their abundance relative to hydrogen is assumed constant. The hydrogen in the expanding envelope is assumed to be all in molecular form. This simplification does not affect the calculated molecular emission, since the CO $J = 1 \rightarrow 0$ line is easily thermalized, and the HCN emission is primarily due to vibrational interaction. Also, at kinetic temperatures of ~ 10 K, as indicated by the CO brightness temperature (Ulich and Haas 1976), the collisional rate between CO and H_2 differs from that between CO and H by less than a factor of 2 (Green and Thaddeus 1976). For both CO and HCN, the rotation collisional rates are interpolated from the tabulated values by Green and Thaddeus (1974, 1976).

Because of the strong infrared continuum of IRC +10216, we have included radiative excitation of CO and HCN from the ground vibrational state to the lowest excited vibrational state. This vibrational interaction increases the excitation of the ground rotational levels as it tends to equilibrate them at a temperature equal to the infrared continuum temperature. Consequently, heating of the gas will also occur when some of these rotational excitations are de-excited by collisions. We neglect, however, the heating that results from collisional de-excitation of the vibrational levels, because this process is very much slower than radiative de-excitation (Thompson 1973). In modeling the infrared properties of IRC +10216, we assume it to be at a distance of 200 pc. The calculated molecular emission can be easily scaled to other distances[1] (cf. § IV). At 4.6 μm, corresponding to the CO $v \rightarrow 1 \rightarrow 0$ wavelength, the continuum is taken to be a 650 K blackbody of radius 6×10^{14} cm (Toombs *et al.* 1972). A vibrational transition moment of 0.1 debye is used (Young and Eachus 1966). Radiative excitation of CO to $v = 2$ and higher vibrational states can be neglected, because of both the fewer continuum photons available at the higher frequencies and the weaker vibrational transition moments. Also neglected in the numerical calculations is the millimeter continuum of the star. The 2.7 K background radiation is included, however, and the brightness temperatures of the millimeter lines calculated always refer to intensities above the background.

For HCN, the lowest excited vibrational state is 715 cm^{-1} above the ground state and is due to the ν_2 bending mode. Infrared observations by Toombs *et al.* indicate that between 10 and 20 μm half of the flux comes from a 650 K blackbody of angular diameter 0.″4, and the remainder comes from an optically thin 2″ shell at a temperature of 350 K. Instead of considering the whole composite source at 15 μm, we assume, for simplicity in the numerical calculations, a single 300 K blackbody of radius 3×10^{15} cm. This simple approximation of the infrared continuum and the uncertainty in the radial velocity gradient both limit the quantitative applicability of the HCN calculations. A transition dipole moment of 0.1 debye (Bruns and Person 1970) is used for the vibrational interaction. This value too is quite uncertain. Radiative excitation at 4.8 μm due to the ν_3 (CN bond) vibrational mode may also contribute to the observed $J = 1 \rightarrow 0$ intensity. The transition moment is weaker by about a factor of 3 (Bruns and Person 1970) than that for the ν_2 mode. This additional interaction has not been included in the numerical calculations.

HCN has hyperfine structure. Each rotational level except $J = 0$ is split into three components. In the numerical calculations this hyperfine structure has not been taken into account in either the ground-vibrational or the excited vibrational state. As far as vibrational transitions are concerned, this simplification is justified because the splittings are smaller than the Doppler widths of the vibration-rotational lines. On the other hand, the splittings are much larger than the Doppler widths of the rotational transitions. Thus, locally, these rotational hyperfine components are separate lines. When hyperfine structure is neglected, the calculated $v = 0$, $J = 1 \rightarrow 0$ intensity equals, in the optically thin regime, the sum of the intensities of the three hyperfine lines were they considered separate components, but would equal only the intensity of each of the three when they are all thermalized. In the numerical calculations we find that, at every point in the envelope, the $J = 1 \rightarrow 0$ intensity never reaches the thermal intensity at the infrared continuum temperature (300 K). Whenever the excitation temperature is high (sometimes greater than 300 K), the opacity is also less than unity. Thus, as far as the total number of photons emitted at each local point in the $J = 1 \rightarrow 0$ transition is concerned, the neglect of hyperfine structure is probably all right. The presence of hyperfine structure in HCN introduces another complication, which is that radiation from the $F = 1 \rightarrow 0$ and $F = 2 \rightarrow 1$ hyperfine transitions will be absorbed along the line of sight due to the $F = 1 \rightarrow 1$ transition. Fortunately, radiative de-excitation (including trapping) is usually faster than collisional de-excitation, and the absorbed photons are mostly reemitted.

III. NUMERICAL RESULTS

The formulation of the multilevel transfer problem in the presence of a velocity gradient was described by Goldreich and Kwan (1974). General expressions for the escape probability for spontaneous emission in a radial flow and for the effective rate of absorption of radiation from a central source were given by Castor (1970). The nonlinear equations for the local level populations of a molecule can be easily derived from the two references above. Only the results of the calculations are presented here.

[1] An approximate distance of 290 pc has been obtained by Herbig and Zappala (1970), based on an estimate of the intrinsic luminosity of the star.

a) *The Temperature Distribution*

The kinetic temperature of the gas is plotted against radius in Figure 1*a*, for a mass loss rate, $\dot{M}$, of $2 \times 10^{-5}\ M_\odot\ \mathrm{yr}^{-1}$, a [CO]/[$H_2$] abundance ratio of 8×10^{-4}, and three values of Q, to illustrate the effect of heating due to gas-dust collisions. The case of $Q = 1.3 \times 10^{-2}$ leads to CO and ^{13}CO emission that best represent the observed line intensities and profiles and will be singled out for discussion. The drift velocity in this case is 2.1 km s^{-1}. The rate of heating per molecule, $n^{-1}dq(\mathrm{dust})/dt$, is 0.74×10^{-25} ergs s^{-1} at 10^{17} cm, to be compared with the cooling rate of -0.46×10^{-25} ergs s^{-1} due to CO emission and that of -0.45×10^{-25} ergs s^{-1} due to free expansion. Only at 3×10^{17} cm does cooling due to expansion begin to dominate over heating due to gas-dust collisions. The importance of this dust heating is further evident in Figure 1*a*, which shows an approximate linear relation between Q and the temperature distribution beyond 10^{17} cm. Neglecting this heating process would lead to a temperature so low in the outer parts of the envelope that it would be difficult to produce the observed CO emission at any mass loss rate.

One check on the appropriateness of the value of Q is provided by calculating the dust opacity. Since Q is approximately the dust absorptivity at 8 μm (the wavelength of peak continuum emission), the dust opacity at this wavelength can be calculated. Infrared observations (Toombs *et al.* 1972) indicate that the continuum emission region has a size of 0".4, which corresponds to a radius of 6×10^{14} cm at a distance of 200 pc. With a mass loss rate of $2 \times 10^{-5}\ M_\odot\ \mathrm{yr}^{-1}$, $Q = 1.3 \times 10^{-2}$, and the other dust properties assumed in § II, the opacity into 6×10^{14} cm is calculated to be unity, which is about what is expected.

The temperature distribution is quite insensitive to variation in the mass loss rate. The rate of heating per molecule due to the gas-dust drift decreases with increasing mass loss rate, but only as $\dot{M}^{-1/2}$. On the other hand, the cooling per molecule due to CO emission, at a fixed [CO]/[H_2] ratio, is less at a higher mass loss rate. This is because at high densities most of the CO rotational transitions are thermalized, and the cooling per unit volume becomes independent of the density. The temperature distribution changes by less than 25% when the mass loss rate varies by a factor of 2. The parameter Q, then, is the dominant factor in determining the kinetic temperature.

The excitation temperature of the CO $J = 1 \rightarrow 0$ line closely follows the kinetic temperature, except at the outer parts of the envelope. For example, in the case of $Q = 1.3 \times 10^{-2}$, $T_{ex}/T_k = 8.1$ K/9.8 K at $r = 10^{17}$ cm where the density is 1.6×10^3 cm^{-3}, but becomes 2.8 K/5.0 K at $r = 4 \times 10^{17}$ cm.

The brightness temperature distributions of the CO line at the central velocity ($v = 0$; henceforth, all velocities v will be referred relative to this central velocity) are also plotted in Figure 1 for the three values of Q. It is evident from the graphs that both the CO emission and the size of the emission region increase with increasing Q, because of the direct

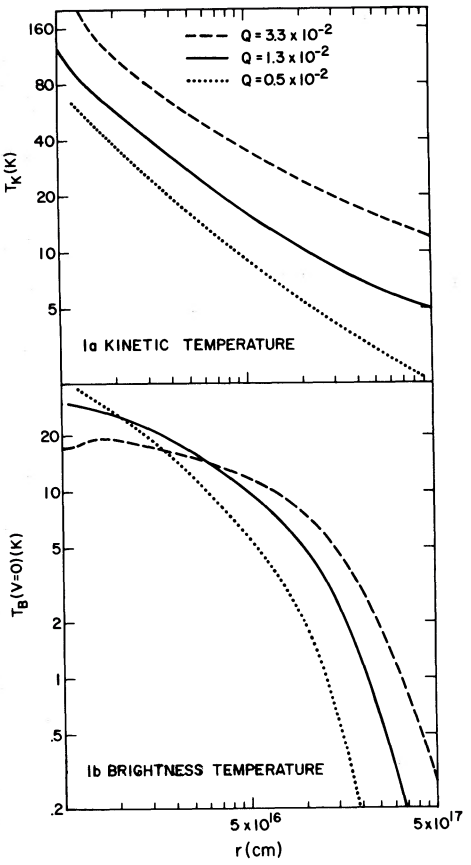

FIG. 1.—The kinetic temperature and the brightness temperature at the central velocity are plotted against radius, for three values of the parameter Q, to illustrate the effect of heating due to gas-dust collisions. A mass loss rate of $2 \times 10^{-5}\ M_\odot\ \mathrm{yr}^{-1}$, and a [CO]/[$H_2$] abundance ratio of 8×10^{-4} are assumed.

relationship between the latter and the kinetic temperature. The graphs also illustrate that very little emission originates from within 2×10^{16} cm. Not only does the surface area decrease more rapidly with decreasing radius than the gas temperature increases, but also the higher temperature distributes the CO molecules over many more rotational levels, so that the $J = 1 \rightarrow 0$ line actually becomes optically thin at inner radii despite the higher densities. The larger velocity gradient at a smaller radius also partly accounts for this decrease in opacity.

b) CO, ^{13}CO $J = 1 \rightarrow 0$ *Emission*

From the brightness temperature distribution of the CO line in Figure 1*b*, the observed antenna temperature at the central velocity can be obtained by convolving this distribution with the antenna pattern. The beam parameters of the NRAO 36 foot (11 m) antenna measured by Ulich and Haas (1976) are adopted, namely, a half-power beamwidth (HPBW) of the main beam of 66″ at 115 GHz and an error beam of 25′. The antenna temperatures at other

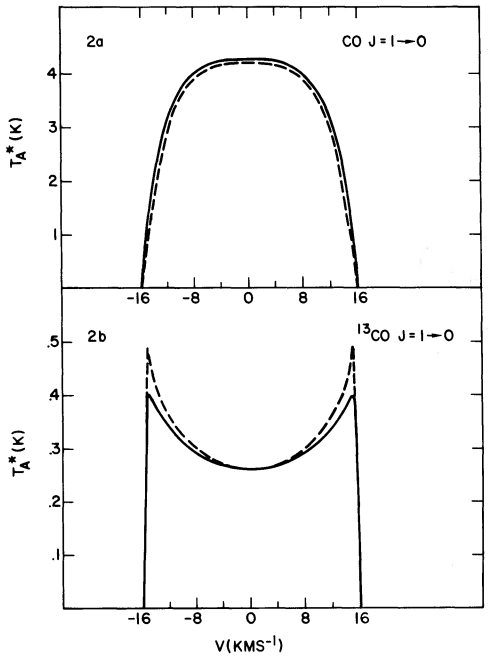

FIG. 2.—The calculated CO and ^{13}CO line profiles (*solid curves*) are compared with the observed profiles (*dashed curves*). The parameters assumed in the calculation are: a distance to the star of 200 pc, a mass loss rate of $2 \times 10^{-5}\ M_\odot\ \mathrm{yr}^{-1}$, a [CO]/[$H_2$] abundance ratio of 8×10^{-4}, a [CO]/[^{13}CO] isotope ratio of 35, and a Q of 1.3×10^{-2}.

velocities can be obtained by appropriate modifications of the line opacity, which depends on both radius and the observed velocity. The resulting line profile for the case of $\dot{M} = 2 \times 10^{-5}\ M_\odot\ \mathrm{yr}^{-1}$, [CO]/[$H_2$] = 8×10^{-4}, and $Q = 1.3 \times 10^{-2}$ is plotted (*solid curve*) in Figure 2*a*. The empirical fit by Kuiper *et al.* (1976) to the observed CO emission is also plotted (*dashed curve*) after it has been normalized to a peak intensity of 4.2 K, as calibrated by Ulich and Haas (1976) after correction for antenna and atmospheric losses. The ^{13}CO line profile is presented in Figure 2*b* (*solid curve*). This is calculated by using the same kinetic temperature distribution and a [CO]/[^{13}CO] abundance ratio of 35. The calculated CO line profile agrees well with the observed profile, but the calculated ^{13}CO line fails to produce as pronounced a double peaking as observed.

For both CO and ^{13}CO, the difference in the emitted intensity is small ($<5\%$) between the case when vibrational excitation is included and the case when it is not. Because of the small permanent dipole moment of CO, even if the $J = 1 \rightarrow 0$ line were optically thin, most of the rotational excitations due to the vibrational interaction would be de-excited by collisions rather than by spontaneous decay.

The different CO and ^{13}CO line shapes manifest the difference between optically thick emission and optically thin emission in a spherically symmetric, uniformly expanding envelope that is partially resolved, as pointed out by Kuiper *et al.* (1976). The optical depth of the CO line at the central velocity is about 2.5 beyond 10^{17} cm and that of the ^{13}CO line about 0.1. Both opacities vary little between 10^{17} cm and 5×10^{17} cm despite the rapid decrease in density from 1800 to 75 cm^{-3}. This is largely due to the decrease in the partition function and the decrease in the velocity gradient.

From the CO brightness temperature distribution in Figure 1*b*, the source size that would be measured by a 66″ antenna can be determined. For the case of $Q = 1.3 \times 10^{-2}$, this size at one-half peak intensity is 100″; the observed value is 140″ (Ulich 1976). This discrepancy in the size is part of the reason for the discrepancy between the calculated and the observed ^{13}CO line profiles, as a larger size would lead to a greater peaking at $v = \pm v_t$. This difficulty in producing the observed size, after fitting the observed CO intensity and line shape, is not dependent on the particular choice of d, $\dot{M}$, or [CO]/[H_2] but is due to the rapid decrease in density with distance, inherent in the assumption of a steady, constant velocity flow. This may indicate that mass loss from IRC +10216 is nonsteady, and occurs in bursts.

In the presence of vibrational excitation, weak maser action in the $J = 1 \rightarrow 0$ line of both CO and ^{13}CO is found near the inner boundary of the envelope in several cases. This maser action results from the difference between the opacity to absorption of the infrared photons from the continuum source and the opacity to the subsequent spontaneous emission (Kwan and Scoville 1974). It is prevalent close to the central source, where the rate of absorption of the infrared photons is high, and at low mass loss rates and low CO abundance so that collisional quenching is unimportant. For the CO $J = 1 \rightarrow 0$ line, maser action is present between 2×10^{15} cm and 5×10^{15} cm in the cases of $\dot{M} \leq 10^{-5}\ M_\odot\ \mathrm{yr}^{-1}$ and [CO]/[H_2] $\leq 3 \cdot 10^{-4}$. The magnitude of the opacity at the central velocity is small (≤ 0.1), however, and the contribution from the maser emission to the total emission at this velocity is completely negligible. Maser action occurs between 2×10^{15} cm and 2×10^{16} cm in the case of ^{13}CO, and at mass loss rates up to $6 \times 10^{-5}\ M_\odot\ \mathrm{yr}^{-1}$, but the magnitude of the opacity at the central velocity is even smaller (<0.03). Because we have postulated the envelope to extend from beyond 2×10^{15} cm, it is not certain that at smaller radii the stronger maser action there might not lead to a large emission along the radial direction (i.e., near $v = \pm v_t$). In this case the line profile might be modified. However, since the emission at the central velocity would not be affected, the conclusion about the [CO]/[^{13}CO] isotope ratio remains valid.

c) HCN, H^{13}CN $J = 1 \rightarrow 0$ *Emission*

Unlike CO and ^{13}CO, the HCN and H^{13}CN $J = 1 \rightarrow 0$ emission is primarily due to vibrational excitation, as Morris (1975) has concluded for the emission of SiS, SiO, CS, and HC_3N. To illustrate this result we have plotted in Figure 3 the antenna temperature at the central velocity (assuming the same telescope parameters at 88 GHz as those at 115 GHz, except for

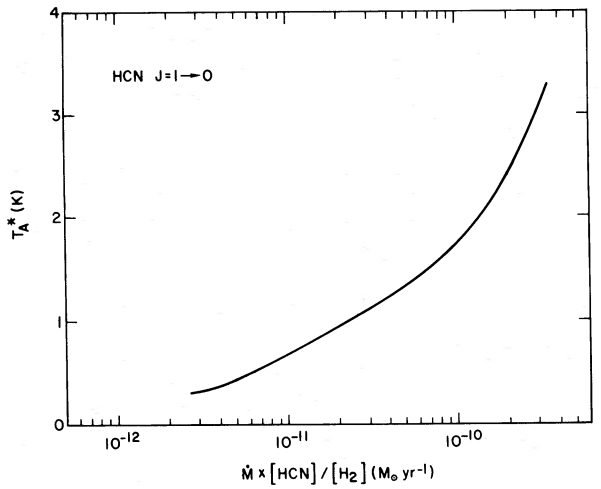

FIG. 3.—Plot of the antenna temperature of the HCN $J = 1 \rightarrow 0$ emission against the absolute HCN density given by $\dot{M} \times [\mathrm{HCN}]/[\mathrm{H_2}]$.

a HPBW of the diffraction beam of 86″ instead of 66″) versus the absolute HCN density, namely, the parameter $\dot{M} \times [\mathrm{HCN}]/[\mathrm{H_2}]$. This curve is insensitive to variation in $\dot{M}$, and points to the fact that the emission depends on neither the H_2 density nor its temperature. The importance of vibrational excitation can be further demonstrated by the fact that, if it were ignored, the same intensity of the emission is obtained only with an abundance of HCN that is almost 50 times greater. The size of the HCN emission region is smaller than that for CO; essentially all the HCN emission originates from within 10^{17} cm.

Because of the strong vibrational interaction, a comment on the effect of the radial velocity distribution we have assumed on the calculated intensities is necessary. Close to the infrared source, the continuum photons are absorbed over a large angle. Even if the velocity were constant along the radial direction, the velocity gradient, when averaged over the solid angle subtended by the central source, would still be large, and the HCN emission in this region would not depend strongly on the radial velocity structure. Far away from the source, the infrared photons are absorbed almost along the radial direction, and when the opacity to their absorption becomes greater than unity (true for HCN), the number of photons absorbed depends directly on the radial velocity gradient. The strong dependence of the HCN emission on the velocity structure, together with our neglect of its hyperfine structure, makes it difficult to compare the calculations with observed quantities. From the observed intensities of HCN and $H^{13}CN$ of 3 K and 1 K, respectively (Gottlieb 1976), we obtain from Figure 3 a $[\mathrm{HCN}]/[\mathrm{H_2}]$ ratio of $\sim 10^{-5}$, and a $[\mathrm{HCN}]/[\mathrm{H^{13}CN}]$ ratio of 13. It is not clear whether the difference between the isotope ratio $[\mathrm{HCN}]/[\mathrm{H^{13}CN}]$ and $[\mathrm{CO}]/[^{13}\mathrm{CO}]$ is real or is a result of the uncertainty in the HCN calculations.

As for CO, weak maser action is also present in the HCN $J = 1 \rightarrow 0$ line, near the continuum source. Again, the magnitude of the opacity at the central velocity is small, and the contribution of the maser emission to the total intensity at this velocity can be neglected, but a better treatment of the maser region, including calculations of the growth of the maser intensity along different directions, will be required in order to determine the contribution of the maser emission to intensities near $\pm v_t$.

IV. DISCUSSION

We have modeled the circumstellar envelope of IRC +10216, assuming a steady, spherically symmetric mass loss from the star. We derive a mass loss rate of $2 \times 10^{-5}\ M_\odot\ \mathrm{yr}^{-1}$, a $[\mathrm{CO}]/[\mathrm{H_2}]$ abundance ratio of 8×10^{-4}, a $[\mathrm{CO}]/[^{13}\mathrm{CO}]$ isotope ratio of 35, and a Q of 1.3×10^{-2}, based on a distance of 200 pc to the star. Here we discuss the uncertainties in these derived results and their dependence on the assumed distance.

At a fixed distance of 200 pc, if the mass loss rate is decreased (increased) from $2 \times 10^{-5}\ M_\odot\ \mathrm{yr}^{-1}$, the $[\mathrm{CO}]/[\mathrm{H_2}]$ ratio would have to be increased (decreased) in order to maintain the same observed intensity. The parameter Q, on the other hand, remains roughly the same since it primarily affects the kinetic temperature through the dust heating, and the latter is quite insensitive to variation in the mass loss rate. Based on these considerations, as well as numerical runs with different parameters, we judge that both $\dot{M}$ and $[\mathrm{CO}]/[\mathrm{H_2}]$ are uncertain to a factor of 2, while Q is uncertain to a factor of 1.2. The uncertainty in the $[\mathrm{CO}]/[^{13}\mathrm{CO}]$ ratio is much smaller, since this ratio can be deduced from a comparison of the CO and ^{13}CO lineshapes alone, quite independent of the other parameters. We estimate this uncertainty to be $\pm 20\%$.

To illustrate the dependence of the derived results on the assumed distance to IRC +10216, we have also performed calculations based on a distance to the star of 290 pc, and obtained $\dot{M} = 4 \times 10^{-5}\ M_\odot\ \mathrm{yr}^{-1}$, $[\mathrm{CO}]/[\mathrm{H_2}] = 6 \times 10^{-4}$, $[\mathrm{CO}]/[^{13}\mathrm{CO}] = 35$, and $Q = 1.8 \times 10^{-2}$. Thus, both $[\mathrm{CO}]/[\mathrm{H_2}]$ and Q are rather insensitive to the assumed distance. The mass loss rate $\dot{M}$, however, varies roughly as the square of the distance. The mass in the circumstellar envelope also depends strongly on the assumed distance. If the mass flow is assumed to extend over an angular diameter of 4′, this mass is 0.14 $M_\odot$ if $d = 200$ pc, and 0.4 $M_\odot$ if $d = 290$ pc.

We can estimate the maximum mass loss rate from IRC +10216 if the acceleration of the flow is due to radiation pressure on grains. Assuming that the primary radiation from the star is all absorbed by the grains in a short distance (which case is likely for IRC +10216) and reradiated isotropically, we have $\dot{M}v_0 = \frac{2}{3}L/c$, where L is the luminosity, and $v_0 = (v_t^2 + v_{\mathrm{esc}}^2)^{1/2}$ is the maximum gas velocity, with v_{esc} the escape velocity at the region where the gas is accelerated. The factor of $\frac{2}{3}$ arises because the acceleration is assumed to occur close to the stellar surface, and only the momentum transfer in the radial direction is utilized. The integrated infrared flux observed is

1.7×10^{-8} W m^{-2} (Becklin *et al.* 1969), so that at a distance of 200 pc the luminosity is $2.1 \times 10^4 L_\odot$. Then, with $v_t = 16$ km s^{-1}, v_{esc} estimated to be 10 km s^{-1}, $\dot{M}$ equals $1.6 \times 10^{-5} M_\odot$ yr^{-1}, which is slightly smaller than the value of $2 \times 10^{-5} M_\odot$ yr^{-1} derived from the CO observations. This approximate equality between the upper limit to the mass loss rate and the derived value is almost independent of the distance to the star, since the former scales as the square of the distance and the latter also approximately so.

We thank Drs. E. Purcell, P. Goldreich, N. Scoville, and J. Theyes for very helpful discussions. We are also grateful to Drs. R. Ulich and C. Gottlieb for communicating their data.

REFERENCES

Becklin, E. E., Frogel, J. A., Hyland, A. R., Kristian, J., and Neugebauer, G. 1969, *Ap. J.* (*Letters*), **158**, L133.
Bruns, R. E., and Person, W. B. 1970, *J. Chem. Phys.*, **53**, 1413.
Castor, J. I. 1970, *M.N.R.A.S.*, **149**, 111.
Dolan, J. F. 1965, *Ap. J.*, **142**, 1621.
Frogel, J. A., Dickinson, D. F., and Hyland, A. R. 1975, *Ap. J.*, **201**, 392.
Geballe, T. R., Wollman, E. R., and Rank, D. M. 1973, *Ap. J.*, **183**, 499.
Gilman, R. C. 1969, *Ap. J.* (*Letters*), **155**, L185.
———. 1972, *Ap. J.*, **178**, 423.
Goldreich, P., and Kwan, J. 1974, *Ap. J.*, **189**, 441.
Goldreich, P., and Scoville, N. 1976, *Ap. J.*, **205**, 144.
Gottlieb, C. A. 1976, private communication.
Green, S., and Thaddeus, P. 1974, *Ap. J.*, **191**, 653.
———. 1976, *Ap. J.*, **205**, 766.
Herbig, G. H., and Zappala, R. R. 1970, *Ap. J.* (*Letters*), **162**, L15.
Herzberg, G. 1966, *Electronic Spectra and Electronic Structure of Polyatomic Molecules* (Princeton, N.J.: Van Nostrand).
Hoyle, F., and Wickramasinghe, N. C. 1962, *M.N.R.A.S.*, **124**, 417.
Kuiper, T. B. H., Knapp, G. R., Knapp, S. L., and Brown, R. L. 1976, *Ap. J.*, **204**, 408.
Kwan, J., and Scoville, N. 1974, *Ap. J.* (*Letters*), **194**, L97.
Morris, M. 1975, *Ap. J.*, **197**, 603.
Mufson, S. L., and Liszt, H. S. 1975, *Ap. J.*, **202**, 183.
Snyder, L. E., and Buhl, D. 1975, *Ap. J.*, **197**, 329.
Thompson, R. I. 1973, *Ap. J.*, **181**, 1039.
Toombs, R. I., Becklin, E. E., Frogel, J. A., Law, S. K., Porter, F. C., and Westphal, J. A. 1972, *Ap. J.* (*Letters*), **173**, L71.
Tsuji, T. 1973, *Astr. Ap.*, **23**, 411.
Ulich, B. L. 1976, private communication.
Ulich, B. L., and Haas, R. W. 1976, *Ap. J. Suppl.*, **30**, 247.
Wilson, W. J., Schwartz, P. R., and Epstein, E. E. 1973, *Ap. J.*, **183**, 871.
Wilson, R. W., Solomon, P. M., Penzias, A. A., and Jefferts, K. B. 1971, *Ap. J.* (*Letters*), **169**, L35.
Young, L. A., and Eachus, W. J. 1966, *J. Chem. Phys.*, **44**, 4195.

F. HILL: Department of Earth and Space Sciences, State University of New York, Stony Brook, NY 11790
J. Y. KWAN: Bell Laboratories, 600 Mountain Avenue, Murray Hill, NJ 07974